JOURNAL OF CATALYSIS 141, 407–418 (1993)

The Effects of Protons on the Hydrogenolysis of Neopentane over Rhodium Catalysts: Rh/HY, Rh/NaHY, and Rh/SiO_2

TIM T. T. WONG AND WOLFGANG M. H. SACHTLER

V.N. Ipatieff Laboratory, Center for Catalysis and Surface Science and Department of Chemical Engineering, Northwestern University, Evanston, Illinois 60208

Received October 15, 1992; revised December 10, 1992

The hydrogenolysis of neopentane (2,2-dimethylpropane) has been studied over the rhodium catalysts Rh/HY, Rh/NaHY, and Rh/SiO_2. The catalytic activity follows the sequence: Rh/HY > Rh/NaHY ≈ Rh/SiO_2. For all catalysts, the conversion of neopentane was 100% selective to hydrogenolysis products, methane, and isobutane; they are formed in a ratio of 1 : 1. In an attempt to determine the true activation energies from the apparent activation energies derived from the Arrhenius curves, corrections were made for the preequilibrium between gaseous and physisorbed neopentane. The adsorption of neopentane on the metal-free supports was determined; isosteric heats of adsorption were calculated from these data. For zeolites NaY and HY they are 8.2 and 7.0 kcal/mol, respectively. After correcting for the preequilibrium, the true activation energies are 33.5 and 38.8 kcal/mol for Rh/HY and Rh/NaHY, respectively. The results lend support to the concept that the superior activity of Rh/HY is due to the "electron deficiency" of the rhodium particles.

INTRODUCTION

Rhodium is one of the most active Group VIII metals for olefin hydrogenation (*1*) and other hydrocarbon reactions, including hydrogenolysis (*2–5*). Assuming that the catalytic activity of transition metals is related to their percentage *d*-bond character as defined by Pauling, Boudart and Ptak attribute the high activity of Rh to the high *d*-bond character of its electrons (*3*). The underlying concept that catalytic activity is correlated to the electronic structure of the metal (*6*) implies that it might be possible to alter catalytic activity by modifying the electronic structure of the metal.

Zeolite-supported metals have been used to probe this concept, since the structure of zeolites not only controls the geometry of the encaged metal particles but has also been claimed to affect their electronic structure. Boudart and co-workers (*7, 8*) reported the turnover frequency of neopentane hydrogenolysis at 272°C to be 44 times higher for Pt supported in CaY than for Pt supported on Al_2O_3. They attribute this enhanced activity to a partial electron transfer from the small (fewer than six atoms) Pt particles to the zeolite support, thereby, creating "electron-deficient" Pt particles. They argue that such Pt clusters will resemble Ir in electronic structure, a metal that has a higher percentage of *d*-bond character and is much more active than Pt for this reaction (*3*).

Homeyer *et al.* (*9, 10*) report a strongly enhanced activity of Pd supported in HY, in comparison to Pd/NaY and Pd/SiO_2. They propose that the increased activity is due to the "electron deficiency" of the Pd particles, caused by an interaction between the reduced metal and the zeolite protons. This interaction leads to the formation of Pd-proton adducts, $[Pd_n\text{–}H_z]^{z+}$ (*11–13*). This model has been tested by several techniques, including infrared spectroscopy of chemisorbed carbon monoxide (*14*), X-ray photoelectron spectroscopy (*15*), and hydrogen isotope exchange (*16*). The results are in agreement that the electron-deficient

0021-9517/93 $5.00

Pd is present in Pd-proton adducts. They do not, however, exclude other causes that might also contribute to the differences in the observed catalytic activity of Pd on various supports. For instance, a preequilibrium of gaseous and physisorbed molecules on the support could lower the apparent activation energy and lead to an increased reaction rate. Furthermore, diffusion must be considered when supports of different porosity are compared.

The objective of the present study is to consider these phenomena in conjunction with the electron deficiency and proton-adduct concepts, which suggest that rhodium supported in a zeolite with a high proton concentration will become similar, in electronic structure, to ruthenium, its left-hand neighbor in the periodic table. Neopentane conversion has been chosen as the test reaction; it is examined over Rh, supported on materials with different proton concentrations, different pore dimensions, and different heats of physical adsorption of neopentane. The catalysts Rh/HY, Rh/NaHY, and Rh/SiO_2 have been prepared and tested, and physical adsorption of neopentane on the metal-free supports has been measured.

EXPERIMENTAL

Sample Preparation

The acidic zeolite HY was prepared by exchanging NaY (LZY-52, Linde) with 10 equivalents of NH_4NO_3 (Aldrich) for each equivalent of NaY in 2000 ml of doubly deionized water. The exchange was performed at room temperature (RT) for 24 h, followed by filtering. This procedure was repeated three times. The NH_4Y sieve was then calcined in a flow of oxygen (50 ml/min/g catalyst), while the temperature was ramped from RT to 500°C over 24 h and held at 500°C for an additional 12 h before cooling to RT.

Before the rhodium was exchanged into the newly formed HY, the zeolite was resaturated with water. This process was accomplished by flowing He (100 ml/min) through a saturator containing doubly deionized water at 11.4°C; this temperature corresponds to a water vapor pressure of 10.1 Torr (1 Torr = 133.3 N/m^2). Water treatment continued until the zeolite was completely resaturated.

Ion exchange of rhodium with NaY or HY was performed by dropwise addition of a dilute solution of $[Rh(NH_3)_5Cl]Cl_2$ to a dilute slurry of the zeolite in doubly deionized water (200 ml/g) at 90°C for 24 h. These conditions permit maximum exchange of Rh; of greater importance is that minimum Cl^- content is achieved, because the equilibrium between $[Rh(NH_3)_5Cl]^{2+}$ and $[Rh(NH_3)_5(H_2O)]^{3+}$ is shifted toward $[Rh(NH_3)_5(H_2O)]^{3+}$ (*17*).

After exchange, the solid was filtered and washed with doubly deionized water until no Cl^- anions were detectable upon addition of $AgNO_3$ to the supernate. Finally, the catalysts were air dried and stored over a saturated NH_4Cl solution in H_2O. The absence of Cl^- was confirmed by XPS.

Davison Grade 62 wide-pore silica gel, 80–100 mesh, was used for the preparation of Rh/SiO_2 by incipient wetness impregnation of $Rh_4(CO)_{12}$ (Strem Chemicals). Details have been previously reported (*18*).

The weight loadings of the catalysts, determined by atomic emission spectroscopy (AES) of inductively-coupled plasma, were 4.0, 4.2, and 1.1 wt% for Rh/HY, Rh/NaHY, and Rh/SiO_2, respectively.

Calcination

For the temperature-programmed reduction or desorption and the catalytic tests, approximately 150 mg of catalyst was used; for measurements of the adsorption of neopentane, approximately 100 mg of catalyst was found sufficient. All samples were first calcined under a high flow (>200 ml/min) of pure oxygen in a packed-bed reactor at atmospheric pressure. The temperature ramp was programmed at 0.5°C/min from RT to the specified calcination temperature (T_c) and held at T_c for 2 h. Oxygen was then replaced by flowing argon (30 ml/min) for 20 min at T_c before cooling to

RT. All further studies were carried out *in situ*.

Temperature-Programmed Reduction and Desorption

Temperature-programmed reduction (TPR) and temperature-programmed desorption (TPD) were used to determine the extent of Rh reduction and the fraction of surface-exposed Rh atoms. The symbol Rh/NaHY is used, in lieu of Rh/NaY, throughout this paper for the reduced rhodium catalyst ion exchanged with NaY because the reduction of the Rh^{3+} cations by hydrogen produces protons.

After calcination, the samples were cooled to −78°C in flowing Ar (30 ml/min) by submerging the reactor into a dry ice/acetone bath. At this temperature, the Ar flow was replaced by a flow (30 ml/min) of H_2 in Ar (5% H_2 in Ar). For TPR, the temperature was ramped from −78°C to the specified reduction temperature (T_R) at 8°C/min and held at T_R for an additional 20 min. The quantity of hydrogen consumed was measured by an on-line thermal conductivity detector and recorded by a computer.

In preparing for TPD, the catalyst was cooled to RT in the H_2 stream to saturate the Rh metal surface with chemisorbed hydrogen. After 15 min, the H_2 flow was replaced with an Ar flow (30 ml/min) and held for an additional 60 min to remove weakly physisorbed hydrogen from the surface of the reactor and catalyst.

Prior to the TPD runs, the reactor was again immersed in the dry ice/acetone bath. The temperature was then ramped from −72°C to 600°C at 8°C/min and held at 600°C for an additional 20 min. The amount of released H_2 was measured by the thermal conductivity detector.

Kinetic Studies, Terminology

Prior to the reaction studies, the samples were reduced in a pure H_2 flow (30 ml/min) at atmospheric pressure. The temperature ramp was, again, programmed at 8°C/min from RT to T_R and held at T_R for 20 min before cooling to the reaction temperature (T_{RXN}).

The reaction of neopentane (2,2-dimethylpropane) with hydrogen was conducted at atmospheric pressure in a continuous-flow packed-bed reactor. A flow of neopentane premixed with hydrogen (1 : 9) was diluted with helium to obtain a neopentane partial pressure of 6 Torr; the overall flow rate was 76 ml/min. Prior to entering the reactor, the reaction mixture was passed through a molecular sieve 5A trap to remove hydrocarbon contaminants.

The reaction products were analyzed by an on-line gas chromatograph (HP 5790, 50-m cross-linked methyl silicone capillary column) equipped with a flame-ionization detector. Since the three catalysts exhibit different activities, different temperature ranges were used to maintain similar conversion ranges; the reaction temperature varied between 100 and 140°C, 120 and 170°C, and 140 and 180°C, for Rh/HY, Rh/NaHY, and Rh/SiO_2, respectively. Throughout the catalytic studies, the conversion level never exceeded 10%; i.e., it remained within the kinetic regime.

For each catalytic run, the temperature was increased by 7°C increments and data were collected at constant temperature. To determine the extent of catalyst deactivation, the temperature was subsequently lowered and additional data were collected. Product distributions were calculated as the carbon percentage of neopentane consumed in the formation of a product.

The turnover frequencies (TOF) reported in this paper are expressed as numbers of neopentane molecules converted per reduced surface rhodium atom every second. The number of reduced surface Rh atoms is evaluated from the ratio of adsorbed H atoms to reduced Rh atoms, H_{ads}/Rh_{red}, derived from TPD and TPR data, respectively. The extent of reduction, Rh_{red}/Rh_{total}, is derived from integration of the TPR profile; it is largely controlled by the local proton concentration of the support (*19, 20*) and, therefore, is different for different supports.

In this paper the notation Rh/*support* (T_C/T_R) will be used to describe the *support* (NaHY, HY, and SiO_2), the calcination temperature (T_C), and the reduction (T_R) temperature of the samples.

Adsorption Measurements

The uptake of neopentane by the metal-free supports (HY, NaY, and SiO_2) was measured using a conventional static adsorption procedure. After calcination, the sample was cooled *in vacuo* (10^{-5} Torr) to the first isotherm temperature; after ca. 60 min the uptake of neopentane was recorded and the presence was increased (the initial neopentane pressures were 1, 2, 3, 5, 7, 10, 15, 20, 30, 50, and 80 Torr). Subsequently, the reactor was evacuated, and the dead volume was determined by expanding Ar. Before the next isotherm was registered at a higher temperature, the sample was degassed *in vacuo* at 350°C. In this way, five adsorption isotherms were registered for each support. Some isotherm measurements were repeated; full reproducibility was found, indicating that no changes in the support structure had occurred during uptake. The isosteric heats of adsorption were calculated from the temperature required to obtain the same coverage at different neopentane pressures.

Mass spectra were also recorded *in situ* during the adsorption and desorption of neopentane using a Dycor M200 quadrupole mass spectrometer. No "cracking" products were detectable with any of the three supports.

RESULTS

Kinetic Studies

Figure 1 shows the Arrhenius curves for Rh/HY(500/300), Rh/NaHY(500/300), and Rh/SiO_2(250/300). Under the present reaction conditions, no deactivation of the catalyst is detectable; the rate of hydrogenolysis and the product distribution observed when returning to the initial reaction temperature are found fully reproducible. This validates the use of neopentane as a probe molecule:

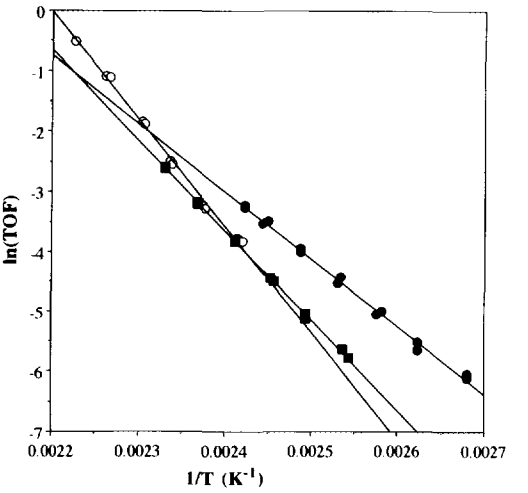

FIG. 1. Arrhenius curves for the hydrogenolysis of neopentane over the following catalysts: Rh/SiO_2 (○); Rh/NaHY (■); and Rh/HY (●).

As it is unable to form olefins or tertiary or secondary carbenium ions in one step, coke formation via such intermediates is minimal. Arrhenius plots are similar for catalysts of different pretreatment history and, therefore, are not shown.

Table 1 lists the turnover frequencies and product distributions at different temperatures for various catalysts. All catalysts in this study displayed 100% selectivity for the hydrogenolysis of neopentane to methane and isobutane, which were always formed in a ratio of 1 : 1. Similar product distributions have been reported for Rh/SiO_2 (*3*). The good reproducibility of the kinetic results permits determination of the apparent activation energy, E_a, and preexponential factor, A, with high accuracy. These parameters are compiled in Table 2. A compensation effect (*21–23*) exists between these kinetic parameters; the linear plot of E_a vs ln(A) is shown in Fig. 2.

Metal-free supports, similarly pretreated as the Rh/NaHY, Rh/HY, and Rh/SiO_2 catalysts, were also tested; they showed no measurable hydrogenolysis of neopentane over the range of reaction temperatures, in-

TABLE 1

Neopentane Hydrogenolysis over Supported Rhodium Catalysts: Product Distributions and Turnover Frequencies[a]

Catalysts	T_R (°C)	T_{RXN} (°C)	Product distributions (%)				TOF[a]
			Me	Et	Pr	iB	
Rh/HY[b]	500	108	19.7	—	—	80.3	3.54e-3
		115	20.5	—	—	79.5	6.92e-3
	400	107	19.2	—	—	80.8	4.65e-3
1		114	19.2	—	—	80.8	8.94e-3
	300	108	21.8	—	—	78.2	4.02e-3
		114	20.9	—	—	79.1	6.72e-3
	200	107.5	21.5	—	—	78.5	3.52e-3
		116	20.8	—	—	79.2	8.18e-3
Rh/NaHY[c]	500	128	20.0	—	—	80.0	7.87e-3
		134.5	22.2	—	2.8	77.5	1.620-2
	400	127	21.2	—	—	78.8	8.69e-3
		134.5	21.7	—	2.7	75.5	1.81e-2
	300	128	21.7	—	—	78.3	6.42e-3
		134.5	22.5	—	—	77.5	1.17e-2
	200	128	24.4	—	—	75.6	4.12e-3
		135	22.5	—	—	77.5	7.18e-2
Rh/SiO_2[d]	500	147	21.9	—	—	78.1	3.21e-2
		156	23.6	—	—	76.4	5.98e-2
	400	147.5	21.5	—	—	78.5	3.13e-2
		154	22.4	—	—	77.6	6.17e-2
	300	148	21.6	—	—	78.4	3.95e-2
		154.5	21.7	—	—	78.3	7.85e-2
	200	147	21.5	—	—	78.5	4.22e-2
		154.5	23.2	—	—	76.8	9.13e-2

[a] Rate expressed in numbers of C5 converted per reduced surface rhodium atom every second.
[b] TC 500°C.
[c] TC 500°C.
[d] TC 250°C.

dicating that the Rh sites are decisive for this catalytic reaction.

Heats of Adsorption

Large amounts of neopentane are adsorbed on NaY and HY at a variety of temperatures. Figures 3 and 4 show the isotherms for the uptake of neopentane; from these isotherms, the heat of adsorption, ΔH, the standard Gibbs free energy of adsorption, $\Delta G°$, and the standard entropy of adsorption, $\Delta S°$, are determined. In contrast to the zeolites, silica adsorbed so little neopentane, even at rather low temperatures, that it was not meaningful to register adsorption isotherms with the same apparatus.

Tables 3 and 4 list the thermodynamic data for neopentane adsorption on zeolites NaY and HY, respectively. By fitting the data to a Langmuir isotherm for nondissociative adsorption, the equilibrium pressure at constant coverage for each temperature was calculated. The heat of adsorption was then determined, at constant coverage, from the Clausius–Clapeyron equation:

TABLE 2

Neopentane Hydrogenolysis over Supported Rhodium Catalysts: Apparent Activation Energies and Preexponential Factors

Catalyst	E_a (kcal/mol)	ln(A)
Rh/HY(500/500)	29.4	33.4
Rh/HY(500/400)	28.8	32.8
Rh/HY(500/300)	22.9	24.4
Rh/HY(500/200)	24.9	27.7
Rh/NaHY(500/500)	32.1	36.1
Rh/NaHY(500/400)	32.1	35.9
Rh/NaHY(500/300)	29.9	32.5
Rh/NaHY(500/200)	28.4	30.4
Rh/SiO_2(250/500)	39.2	42.4
Rh/SiO_2(250/400)	37.9	42.0
Rh/SiO_2(250/300)	35.9	38.8
Rh/SiO_2(250/200)	35.7	40.6

$$[d \ln(P_{eq})/dT]_\theta = -\Delta H/RT^2. \quad (1)$$

The coverage, θ, for the catalyst was chosen to be comparable to that of the catalytic tests. The isosteric heats of adsorption of neopentane for NaY and HY are 8.2 and 7.0 kcal/mol, respectively (1 kcal = 4.184 kJ).

From these calculated heats and the established isotherms, the Gibbs free energy and the entropy of adsorption were calculated from first principles:

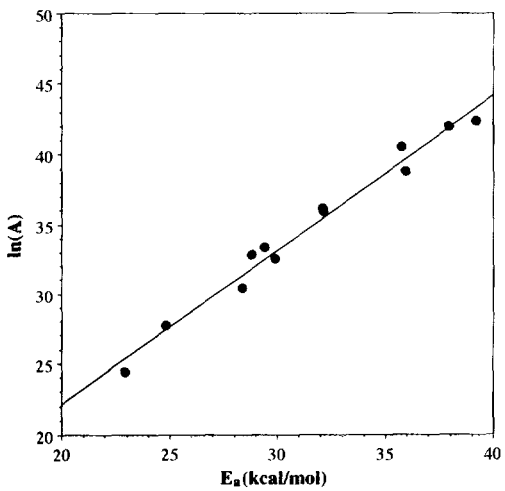

FIG. 2. Compensation effect in the hydrogenolysis of neopentane over supported rhodium catalysts.

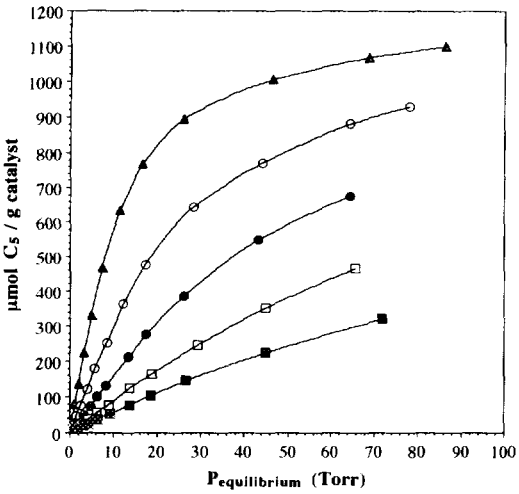

FIG. 3. Neopentane adsorption isotherms on zeolite NaY, after calcination to 500°C. (▲) 100°C; (○) 125°C; (●) 150°C; (□) 175°C; (■) 200°C.

$$\Delta G^\circ = -RT \ln\{[\theta/(1-\theta)]P^\circ/P\} \quad (2)$$

$$\Delta G^\circ = \Delta H - T\Delta S^\circ. \quad (3)$$

The standard state is defined as P° = 1 atm and θ = 0.5. A more descriptive summary

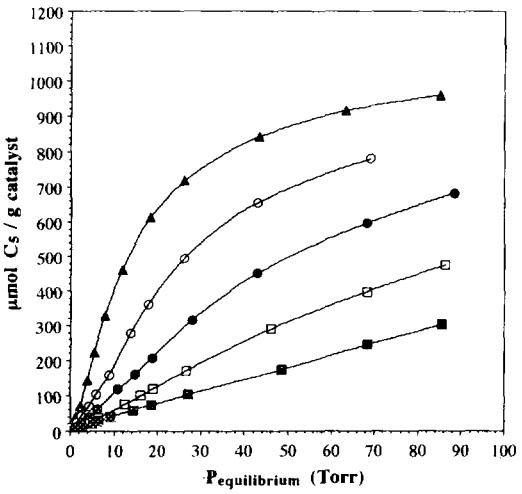

FIG. 4. Neopentane adsorption isotherms on zeolite HY, after calcination to 500°C. (▲) 100°C; (○) 125°C; (●) 150°C; (□) 175°C; (■) 200°C.

TABLE 3

Thermodynamic Data for Neopentane Adsorption on Zeolite NaY after Calcination to 500°C

Temperature (°C)	$-\Delta H$ (kcal/mol)	$-\Delta G^\circ$ (kcal/mol)	$-\Delta S^\circ$ (cal/mol K)
100	8.2	4.2	10.8
125	8.2	4.0	10.6
150	8.2	3.8	10.0
175	8.2	3.2	11.1
200	8.2	3.1	10.7

of the data analysis has been reported by Eberly (*24*).

DISCUSSION

The results of this study provide a clear pattern of the catalytic behavior of supported rhodium catalysts for the hydrogenolysis of neopentane. The catalytic activity over the three catalysts follows the sequence: Rh/HY > Rh/NaHY ≈ Rh/SiO_2 (see Fig. 1); the activation energy, E_a, decreases as the proton concentration of the support increases (see Table 2). The apparent activation energies are 26.5, 30.6, and 37.2 kcal/mol for Rh/HY, Rh/NaHY, and Rh/SiO_2, respectively; within experimental error, they are independent of the pretreatment conditions.

Three possible causes will be considered for these relations: (1) adsorption equilibrium, (2) pore diffusion limitations, and (3) electronic modification of the metal sites.

TABLE 4

Thermodynamic Data for Neopentane Adsorption on Zeolite HY after Calcination to 500°C

Temperature (°C)	$-\Delta H$ (kcal/mol)	$-\Delta G^\circ$ (kcal/mol)	$-\Delta S^\circ$ (cal/mol K)
100	7.0	4.5	6.8
125	7.0	4.3	6.7
150	7.0	4.2	6.9
175	7.0	3.5	7.8
200	7.0	3.8	6.8

Adsorption Equilibrium

Presumably, the transition state of the adsorbed neopentane molecule on the rhodium will be reached from a precursor state in which the molecule is also adsorbed on the rhodium. If this precursor state is in equilibrium with physisorbed neopentane on the support, we can use either the gas phase or the physisorbed state as reference for the enthalpy of the transition state. It has been argued that physisorption of reactants on the catalyst will lead to lowering of the apparent activation energy, thus being one of the causes for the compensation effect as first described by Schwab (*21*) and Cremer (*22*).

Recent work by Haag on hexane cracking over various acid zeolites is consistent with this view (*25*). Differences in the apparent activation energy were noted, ranging from 37 kcal/mol for US-Y to 30 kcal/mol for ZSM-5 to 27 kcal/mol for ZSM-23. When the apparent activation energies were corrected for the heats of physical adsorption of hexane on these zeolites (12, 19, and 23 kcal/ml for US-Y, ZSM-5, and ZSM-23, respectively), using

$$E_{\text{intrinsic}} = E_a - \Delta H, \qquad (4)$$

it appeared that the true activation energy, $E_{\text{intrinsic}}$, was equal for the three catalysts. In this definition, $E_{\text{intrinsic}}$ is the enthalpy difference between the transition state and the physisorbed molecule, but E_a is the enthalpy difference between the transition state and the gas-phase molecule. Although application of such formalism to the present reaction might be debatable, it is of interest to separate possible effects of different heats of physisorption from other causes for the observed differences of the apparent activation energy. Application of Eq. (4) to the present data leads to the following values for $E_{\text{intrinsic}}$:

Rh/HY, 33.5 kcal/mol;

Rh/NaHY, 38.8 kcal/mol.

For Rh/SiO_2, the low uptake of neopentane did not permit us to derive a number for the

heat of physical adsorption; we can only state that the intrinsic activation energy of Rh/SiO_2 should be larger than 37.2 kcal/mol. The heat of adsorption measured in this study for neopentane on NaY is quite similar to that reported by Bülow *et al.* (*26*) for neopentane on NaX (9.9 kcal/mol); trivial experimental errors are, therefore, unlikely.

The important conclusion is that correction for preequilibrium, as given by Eq. (4), does *not* eliminate the differences in activation energies, but actually accentuates them. Since the heat of physical adsorption is larger on NaY than on HY, the difference in the catalytic activity between Rh/NaHY and Rh/HY, therefore, becomes even more pronounced. The apparent activation energies for Rh/HY and Rh/NaHY differ by approximately 4 kcal/mol; after the correction the difference is 5.3 kcal/mol.

Pore Diffusion Limitations

Pore diffusion control would lower the apparent activation energy. It is, however, unlikely that this phenomenon could explain the observed differences in activation energies and turnover frequencies since the pore dimensions and tortuosity are very similar for the two zeolites, but different in SiO_2. The data show that Rh/NaY and Rh/SiO_2 have very similar activation energies, whereas Rh/HY displays a much lower value. Pore diffusion control implies that the measured reaction rate is lower than the intrinsic rate in the absence of pore diffusion control. Moreover, it is not reasonable to assume that pore diffusion limitations would be more severe for the wide pores of SiO_2 than for the narrow channels of zeolite Y. We thus conclude that pore diffusion control cannot be the prevailing cause for the observed differences in activity and true activation energy.

This conclusion is further supported by a kinetic analysis based on the Weisz–Prater criterion (*27*), using data published by Yao and Shelef (*5*) for the reaction order of neopentane hydrogenolysis over Rh/Al_2O_3 (first order with respect to the partial pressure of neopentane), and data published by Bülow *et al.* (*26*) for the diffusion of neopentane into zeolite NaX. We refrain from reporting this analysis in detail in the present paper.

From the above arguments, we conclude that the pronounced differences in the intrinsic activation energy, between rhodium on a support with a high proton concentration and rhodium on supports with low proton concentrations, reflect a genuine modification of the Rh sites.

Metal–Proton Interactions

Two kinds of interactions between reduced Rh clusters in zeolite cages and zeolite protons can be visualized.

Model A. In analogy to the results found previously with Pd/NaHY and Pd/HY samples, an adduct between transition metal cluster and zeolite protons can be formed (*16*). For rhodium, this would be written as $[Rh_n\text{–}H_2]^{2+}$, whereby the protons are assumed to bridge between the metal atoms and the oxygen atoms of the cage wall: vis-à-vis, Rh–H–O. The positive charge is, subsequently, shared between the metal atoms and the hydrogen atoms.

In the case of Pd, this positive charge on the metal was derived from the shift in the binding energy measured by XPS (*15*). Moreover, utilizing infrared spectroscopy, the attachment of protons to the metal was identified. In particular, upon admission of carbon monoxide to the reduced Pd particles, the carbon monoxide displaces most of the protons from the metal cluster; this process, in turn, leads to an increase in the intensity of the IR band characteristic for zeolitic hydroxyl, O–H, groups (*14*). Apparently, some protons still remain attached to the metal cluster because the remaining positive charge results in a blue shift of the CO absorption frequency, as reported by Figueras *et al.* (*28*) and Zhang *et al.* (*14*). This blue shift indicates an increase in the force constant between the carbon and the oxygen atoms of CO; this is caused by the decrease in the back-donation of the *d*-elec-

trons of the electron-deficient metal into the vacant carbon monoxide π^* orbital.

The bridging proton in the palladium-proton adduct also acts as a chemical anchor; removing the anchor by admitting CO (*29*), hydrocarbons or ammonia (*30*) leads to an agglomeration of the palladium clusters. As the formation of the palladium-proton adduct results in a lowering of the activation energy for neopentane conversion, and in a significant decrease of the activation energy of that reaction (*9*), it seems reasonable to assume that the same model is also valid for Rh in Rh/HY.

Model B. The reduction with hydrogen of zeolite-encaged transition metal ions

$$M^{z+} + z/2H_2 = M^\circ + zH^+ \qquad (5)$$

leads to an equilibrium, which is shifted far to the right for metals such as Pt and Pd; only isolated atoms can be reoxidized by protons (*31–34*). For Rh, however, the situation is different; our previous data show that reduction remains incomplete unless the protons formed in (5) are neutralized (*19, 20*). Presumably, some of the unreduced Rh cations will be located in the small zeolite cages; but, as the proton concentration increases, some unreduced Rh cations will be present in the supercages. Consequently, the Rh_n clusters formed in HY share their cages not only with protons, but also with Rh cations, presumably Rh^+. The interaction between a reduced Rh_n cluster and an unreduced Rh^+ cation in the same cage; i.e.,

$$Rh_n + Rh^+ \Rightarrow [Rh_{n+1}]^+ \qquad (6)$$

will give rise to a larger cluster of $n + 1$ atoms, carrying a net positive charge. Although this positive charge will be delocalized over the entire cluster, the local charge density will be highest near the negative charge in the cage wall.

This interaction between reduced metal particles and unreduced cations has been claimed to be responsible for anchoring metals on oxide supports. For Pt/Al_2O_3, Huizinga and Prins (*35*) reported on ESR results and showed a direct interaction between unreduced Pt^+ cations and reduced Pt particles. These cations are situated at the metal/support interface, anchoring the Pt particles to the oxide support. This phenomenon has also been studied with bimetallic catalysts, where the reduced metal particles are anchored by cations of different elements. Tzou *et al.* (*36*) reported on EXAFS evidence for the anchoring of Rh particles by Cr cations. In the case of RhFe/NaY, Mössbauer and EXAFS results indicate chemical bonding between reduced Rh and the Fe^{3+} cations (*37*). In addition to anchoring, this interaction has been proposed to promote the activity for syngas conversion (*36, 38–40*) and olefin hydroformylation (*41*).

The common features of Models A and B is the partial positive charge on the Rh atoms that serve as sites for adsorption and catalysis. It is essential, however, to recognize that Model A emphasizes the proton to reduced Rh ratio, (H^+/Rh°), whereas Model B emphasizes the Rh cation to reduced Rh ratio, (Rh^+/Rh°).

An estimate of the (H^+/Rh°) ratio can be made. Rh/SiO_2 contains essentially no protons, but Rh/HY contains approximately 56 protons per unit cell. Rh/NaHY, however, has an upper limit of 21 protons per unit cell, assuming 100% reduction of Rh^{3+} to Rh°. The actual proton concentration will be much lower, as part of the Rh is incompletely reduced.

An estimate of the (Rh^+/Rh°) ratio can also be made. After ion exchange approximately, 7 Rh^{3+} cations per unit cell are present in both Rh/HY and Rh/NaHY. The percentage reduction of Rh^{3+} is only slightly greater in Rh/NaHY than in Rh/HY, indicating only a small difference in the (Rh^+/Rh°) ratio for the two zeolite samples. For Rh/SiO_2, however, the percentage reduction is near 100%; i.e., the (Rh^+/Rh°) ratio is essentially zero.

It follows that the ratios, (H^+/Rh°) and (Rh^+/Rh°), correlate differently: (H^+/Rh°) follows the sequence Rh/HY > Rh/NaHY $\approx$ Rh/SiO_2, whereas (Rh^+/Rh°) follows the

sequence Rh/HY ≈ Rh/NaHY ≫ Rh/SiO_2. It appears that the sequence of the catalytic activities correlates better with Model A than with Model B, as the activity difference between Rh/HY and the other samples is much more pronounced than the difference between Rh/NaHY and Rh/SiO_2. We therefore assume that the formation of metal-proton adducts is the major cause of the electron deficiency resulting in a lower activation energy and a higher rate for the conversion of neopentane.

The activity of Ru, the left-hand neighbor of Rh in the Periodic Table, for hydrogenolysis of neopentane (*3*) or ethane (*42*, *43*) is higher than that of Rh. This lends justification to the statement that electron-deficient Rh resembles Ru in electronic structure. This is analogous to previous statements that electron-deficient Pd (*44*) and Pt (*45–50*) are similar to their left-hand neighbors.

A similar trend was reported by Figueras *et al.* (*28*) for the hydrogenation of benzene over supported Pd catalysts. They found that the catalytic activity increased with an increase in the support acidity, i.e., LaY ≈ HY ≈ CeY > MgY > CaY > NaY > NaX, and concluded that an electron transfer makes the electronic configuration of Pd particles similar to that of Rh particles.

The statement that electron withdrawal makes transition metal clusters similar to their left-hand neighbors is not meant to be a resurrection of alchemistic attempts to transform elements into other elements; it is merely a consequence of the fact that the electronic structure and orbital filling are essential for the strength of chemical bonds.

An electronic metal/support interaction had been proposed in the past for much larger particles of transition metals on amorphous supports. This early speculation was found in contradiction with experimental evidence. For large particles on a planar support, the metal/solid interface is not identical to that of the metal/gas interface; the atoms of the latter interface are shielded from electron transitions between metal and support (*51*). For the much smaller particles located in almost spherical zeolite cages, this shielding is less effective; adsorbing atoms will often be the first neighbors of metal atoms to form a chemical bond, e.g., with a zeolite "proton."

Jansen and van Santen (*52*) have shown, for Ir_4 clusters in a zeolite, that the polarization due to a Mg^{2+} cation will also affect the Ir atom, which is only the second neighbor to the Mg^{2+} cation. This interaction is reflected in the pronounced modification of its bond to an adsorbed CO molecule. In the same light, it is conceivable that Rh atoms in a small cluster carrying a positive charge will display chemisorption and catalytic characteristics different from those of exactly neutral Rh clusters.

CONCLUSIONS

1. The supported Rh catalysts are 100% selective for the hydrogenolysis of neopentane to methane and isobutane. Their catalytic activity decreases in the order: Rh/HY > Rh/NaHY ≈ Rh/SiO_2.
2. The superior activity of Rh in a zeolite with high proton concentration is tentatively attributed to the formation of electron-deficient rhodium metal particles.
3. Apparent activation energies have been measured with high accuracy; after correcting for the enthalpy of adsorption, the intrinsic activation energies are significantly different for zeolite supports of different proton concentration.

ACKNOWLEDGMENTS

Final support by the National Science Foundation, Contract CTS-8911184/02, is gratefully acknowledged. T.T.T.W. thanks the International Precious Metals Institute for financial support. We also thank W. Haag for very helpful and clarifying discussions. The assistance of G.-D. Lei in the adsorption measurements is gratefully acknowledged. We thank Johnson Matthey, Ltd., for providing $RhCl_3$ in their precious metal loan program and we thank J. B. Butt and Z. Karpiński for providing the Rh/SiO_2 sample used in this study.

REFERENCES

1. Beeck, O., *Discuss. Faraday Soc.* **8**, 118 (1950).
2. Yates, D. J. C., and Sinfelt, J. H., *J. Catal.* **8**, 348 (1967).

3. Boudart, M., and Ptak, L. D., *J. Catal.* **16,** 90 (1970).
4. Coq, B., Dutartre, R., Figueras, F., and Tazi, T., *J. Catal.* **122,** 438 (1990).
5. Yao, H. C., and Shelef, M., *J. Catal.* **56,** 12 (1979).
6. Boudart, M., *J. Am. Chem. Soc.* **72,** 1040 (1950).
7. Dalla Betta, R. A., and Boudart, M., *in* "Proceedings, 5th International Congress on Catalysis, Palm Beach, 1972" (J. W. Hightower, Ed.), p. 1329. North-Holland, Amsterdam, 1973.
8. Boudart, M., Aldag, A. W., Ptak, L. D., and Benson, J. E., *J. Catal.* **11,** 35 (1968).
9. Homeyer, S. T., Karpiński, Z., and Sachtler, W. M. H., *Rec. Trav. Chim. Pays-Bas* **109,** 81 (1990).
10. Homeyer, S. T., Karpiński, Z., and Sachtler, W. M. H., *J. Catal.* **123,** 60 (1990).
11. Sachtler, W. M. H., *in* "Chemistry and Physics of Solid Surfaces" (R. Vanselov and R. Howe, Eds.), p. 69, Springer Series in Surface Science 22. Springer-Verlag Berlin, 1990.
12. Karpiński, Z., Homeyer, S. T., and Sachtler, W. M. H., *in* "Studies in Surface Science and Catalysis" (R. K. Grasselli and A. Slaught, Eds.), p. 67. Elsevier, Amsterdam, 1991.
13. Sachtler, W. M. H., and Stakheev, A. Y., *Catal. Today* **12,** 283 (1992).
14. Zhang, Z., Wong, T. T. T., and Sachtler, W. M. H., *J. Catal.* **128,** 13 (1991).
15. Stakheev, A. Y., and Sachtler, W. M. H., *J Chem. Soc. Faraday Trans.* **87**(22), 3703 (1992).
16. Xu, L., Zhang, Z., and Sachtler, W. M. H., *J. Chem. Soc. Faraday Trans.* **88**(15), 2291 (1992).
17. Shannon, R. D., Vedrine, J. C., Naccache, C., and Lefebvre, F., *J. Catal.* **88,** 431 (1984).
18. Karpiński, Z., Chuang, T.-K., Katsuzawa, H., Butt, J. B., Burwell, R. L., Jr., and Cohen, J. B., *J. Catal.* **99,** 184 (1986).
19. Wong, T. T. T., Zhang, Z., and Sachtler, W. M. H., *Catal. Lett.* **4,** 365 (1990).
20. Wong, T. T. T., Stakheev, A. Y., and Sachtler, W. M. H., *J. Phys. Chem.* **96,** 7733 (1992).
21. Schwab, G.-M., *in* "Advances in Catalysis" (W. G. Frankenburg, V. I. Komarewsky, and E. K. Rideal, Eds.), Vol. 2, p. 251. Academic Press, New York, 1950.
22. Cremer, E., *in* "Advances in Catalysis" (W. G. Frankenburg, V. I. Komarewsky, and E. K. Rideal, Eds.), Vol. 7, p. 75. Academic Press, New York, 1955.
23. Galwey, A. K., *in* "Advances in Catalysis" (D. D. Eley, H. Pines, and P. B. Weisz, Eds.), Vol. 26, p. 247. Academic Press, New York, 1977.
24. Eberly, P. E., Jr., *J. Phys. Chem.* **67,** 2404 (1963).
25. Haag, W., personal communication, Ipatieff Lectureship, Northwestern University, 1992.
26. Bülow, M., Lorenz, P., Mietke, W., and Struve, P., *J. Chem. Soc. Faraday Trans.* **79,** 1099 (1983).
27. Weisz, P. B., and Prater, *in* "Advances in Catalysis" (W. G. Frankenburg, V. I. Komarewsky, and E. K. Rideal, Eds.), Vol. 6, p. 143. Academic Press, New York, 1954.
28. Figueras, F., Gomez, R., and Primet, M., *in* "Molecular Sieves" (W. M. Meier and J. B. Uytterhoeven, Eds.), Adv. Chem. Ser., Vol. 121, p. 480, 1973.
29. Zhang, Z., Chen, H., Sheu, L.-L., and Sachtler, W. M. H., *J. Catal.* **127,** 213 (1991).
30. Zhang, Z., Lerner, B., Lei, G.-D., and Sachtler, W. M. H., *J. Catal.* **140,** 481 (1993).
31. Tzou, M. K., Teo, B. K., and Sachtler, W. M. H., *J. Catal.* **113,** 220 (1988).
32. Tzou, M. K., Kusunoki, M., Asakura, K., Kuroda, H., Moretti, G., and Sachtler, W. M. H., *J. Phys. Chem.* **95,** 5210 (1991).
33. Zhang, Z., Xu, L., and Sachtler, W. M. H., *J. Catal.* **131,** 502 (1991).
34. Feeley, J. S., Stakheev, A. Y., Cavalcanti, F. A. P., and Sachtler, W. M. H., *J. Catal.* **136,** 182 (1992).
35. Huizinga, T., and Prins, R., *J. Phys. Chem.* **87,** 173 (1983).
36. Tzou, M. S., Teo, B. K., and Sachtler, W. M. H., *Langmuir* **2,** 773 (1986).
37. Fukuoka, A., Kimura, T., Rao, L.-F., and Ichikawa, M., *Catal. Today* **6,** 55 (1989).
38. Ichikawa, M., *Polyhedron* **7**(22/23), 2351 (1988).
39. Ichikawa, M., Shriver, D. F., Lang, A. J., and Sachtler, W. M. H., *J. Am. Chem. Soc.* **107,** 7216 (1985).
40. Van Den Berg, F. G. A., Glezer, J. H. E., and Sachtler, W. M. H., *J. Catal.* **93,** 340 (1985).
41. Fukuoka, A., Rao, L.-F., Kosugi, N., Kuroda, H., and Ichikawa, M., *Appl. Catal.* **50,** 295 (1989).
42. Sinfelt, J. H., and Yates, D. J. C., *J. Catal.* **8,** 82 (1967).
43. Yates, D. J. C., and Sinfelt, J. H., *J. Catal.* **14,** 182 (1969).
44. Juszczyk, W., Karpiński, Z., Ratajczykowa, I., Stanasiuk, Z., Zieliński, J., Sheu, L.-L., and Sachtler, W. M. H., *J. Catal.* **120,** 68 (1989).
45. Gallezot, P., Datka, J., Massardier, J., Primet, M., and Imelik, B., *in* "Proceedings, 6th International Congress on Catalysis, London, 1976" (G. C. Bond, P. B. Wells, and F. C. Tompkins, Eds.), Vol. 2, p. 696. The Chemical Society, London, 1977.
46. Tri, T. M., Massardier, J., Gallezot, P., and Imelik, B., *in* "Proceedings, 7th International Congress on Catalysis, Tokyo, 1980" (T. Seiyama and K. Tanabe, Eds.), p. 266. Elsevier, Amsterdam, 1981.
47. Naccache, C., Kaufherr, N., Dufaux, M., Bandiera, J., and Imelik, B., *in* "Molecular Sieves II, Proceedings, 4th International Congress on Molecular Sieves, University of Chicago, 1977" (J. R. Katzer, Ed.), p. 538. American Chemical Society, Washington, 1977.

48. Gallezot, P., *Catal. Rev. Sci. Eng.* **20**(1), 121 (1979).
49. Figueras, F., Mencier, B., De Mourgues, L., Naccache, C., and Trambouze, Y., *J. Catal.* **19,** 315 (1970).
50. Foger, K., and Anderson, J. R., *J. Catal.* **54,** 318 (1978).
51. Ponec, V., *in* "Proceedings, 9th International Vacuum Congress–International Conference on Solid Surfaces, Madrid, Spain, 1983" (J. L. De Segovia, Ed.), p. 121. Asoc. Esp. Vacio Sus Apl., Madrid, Spain, 1983.
52. Jansen, A. P. J., and van Santen, R. A., *J. Phys. Chem.* **94,** 6764 (1990).